JOURNAL OF CATALYSIS 137, 22–35 (1992)

Reaction Analysis of Potassium Promotion of Ru-Catalyzed CO Hydrogenation Using Steady-State Isotopic Transients

T. E. HOOST[1] AND J. G. GOODWIN, JR.[2]

Chemical and Petroleum Engineering Department, University of Pittsburgh, Pittsburgh, Pennsylvania 15261

Received April 24, 1991; revised March 3, 1992

The effects of alkali on catalyst activity and deactivation during CO hydrogenation have been studied in the past mostly based on an available surface-metal atoms approach. However, such an approach cannot easily distinguish to what extent the modifier brings about changes in surface concentrations of reaction intermediates or affects site activity during steady-state reaction. Steady-state isotopic transient analysis (SSITKA) with carbon tracing was used to decouple the effects of potassium on the methane-producing sites during steady-state CO hydrogenation over Ru/SiO_2 catalysts having modifier loadings of up to $(K/Ru)_{atom} = 0.2$. The SSITKA results indicate that, during steady-state CO hydrogenation, carbidic carbon evolved into methane via a high-reactivity ($C_{1\alpha}$) and a low-reactivity ($C_{1\beta}$) trajectory. With increasing amounts of K^+ the average "true" intrinsic turnover frequency (k) of both of these carbidic pools decreased, as did their steady-state surface abundance. Relative to $C_{1\beta}$, the $C_{1\alpha}$ pool was affected to a slightly greater extent, both in terms of its reactivity and abundance. It is likely that potassium was able to strengthen the carbon–metal interaction which made hydrogenation of the carbon adlayer more difficult, resulting in smaller methane-destined pools of active surface carbon. With time-on-stream, deactivation by deposition of inactive carbon did not significantly affect the product distribution or the methane rate constant at the prevailing K^+ doping levels; instead, deactivation was due to a loss in the steady-state abundance of carbon-containing surface intermediates exiting as methane. Implications of the role of potassium during steady-state CO hydrogenation in influencing the active metal surface, the carbidic adlayer, and the latter's transformation into unreactive carbon are addressed.

1. INTRODUCTION

Chemical modification of CO hydrogenation catalysts with alkali addition has been shown to be effective in improving the selectivity for higher hydrocarbons (*1*). It is evident that the alkali promoter typically decreases rates of formation of all the products but that methane formation is affected more dramatically resulting in an increase in higher-hydrocarbon selectivity. This decrease in rates is often ascribed to a decrease in the catalyst's hydrogenation function upon alkali addition (*2, 3*).

In Fischer–Tropsch synthesis one of the most difficult problems has been the elucidation of the mechanism(s) of alkali promotion. In particular, the means by which the alkali modifier may affect the carbidic[3] adlayer under practical reaction conditions has remained mostly unclear. Many surface-science studies show that for CO adsorption on alkali-metal promoted, single-crystal metal surfaces, the C–M bond is further strengthened while the C–O bond is weakened with promotion, possibly due to electron enrichment of the surface by charge donation from the modifier and attendant electrostatic field effects of the (partially)

[1] Current address: Research Staff, Ford Motor Company, P.O. Box 2053, Dearborn, MI 48121.

[2] To whom correspondence should be addressed.

[3] "Carbidic," as has been suggested by Biloen (*4*), is used here as a collective adjective for a family of reactive surface species C_xH_y, which do not contain oxygen.

0021-9517/92 $5.00

ionized modifier (*5*). For the addition of univalent alkali, electrostatic field effects are suggested to bear primary responsibility for the changes brought about by the modifier (*6, 7*). Thus, according to such an electrostatic approach, alkali promotion results in increased CO dissociation but more tightly bound surface carbon (*8*). An infrared study of CO adsorption on the series of K^+-doped Ru catalysts studied here showed results consistent with such an approach (*9*). In the context of the CO hydrogenation reaction, the influence of alkali on the dissociative CO adsorption is thought to be responsible for the observed increases in the selectivity for higher hydrocarbons, the increase in the olefinic content of the products, and, more generally, the decrease in the hydrogenation rate of carbon (*2, 3*).

It is well known that during CO hydrogenation there is a large pool of reversibly adsorbed CO which occupies a large portion of the metal surface while not participating in the reaction directly (*10*). Traditionally, rate results in kinetic studies of the CO hydrogenation reaction have been presented on a global or on an available surface-metal atoms basis. Using such an approach, one is not able to handle/deconvolute the simultaneous effects that the promoter may have on the abundance of active sites and their "true" intrinsic site turnover frequency, the apparent first-order reaction rate constant k.

In this study we utilized steady-state isotopic transient kinetic analysis (SSITKA) to deconvolute the global methane formation rate into the abundance (N_{CH4}) of the carbon-containing reaction intermediates leading to methane and their intrinsic turnover frequency (k_{CH4}). We were able to determine to what extent alkali promotion was able to bring about actual site modification for those sites producing methane—the product that is usually most drastically affected by alkali promotion for ruthenium-catalyzed CO hydrogenation. Figure 1 schematically shows the pathways traced isotopically during steady-state reaction; surface trajectories of higher hydrocarbons were not traced but their exit into the gas phase was monitored. How alkali promotion may affect catalyst deactivation by inactive carbon was also explored.

2. EXPERIMENTAL

2.1. Catalyst Preparation and Characterization

The preparation procedure for the catalysts has been described elsewhere (*11*). Briefly, portions of a pre-reduced, prewashed, chlorine-free 3 wt% Ru/SiO_2 base catalyst were sequentially impregnated with potassium nitrate solutions of different concentrations. After drying, these catalysts were re-reduced at 400°C. The catalysts were named K*xx* or s*Kxx*, where *xx* indicates that nominally $(K/Ru)_{atom} = xx/100$ and s designates catalysts prepared from a second batch of base catalyst. Although sequential doping may not be the most effective way to achieve intimate modifier–metal interaction, it has been found useful (*12–14*) since it allows one to study the chemical modification of catalysts in the absence of complicating factors, such as particle-size changes, that typically result when doped metal catalysts are prepared by co-impregnation.

Previous characterization (*11*) of this sequentially promoted catalyst series showed that the potassium was apparently located exclusively on the metal surface, where it affected static hydrogen chemisorption on a one-to-one atomic basis. Ethane hydrogenolysis results as indicated that with increasing potassium levels the potassium dispersion became nonuniform (*11*). Some pertinent characteristics of the series are shown in Table 1. Even though other mechanisms cannot be excluded altogether, the stronger linear correlation between added potassium and the ruthenium atoms that were unavailable upon potassium addition as measured by hydrogen chemisorption suggests that simple site blocking by the potassium compound was the most likely

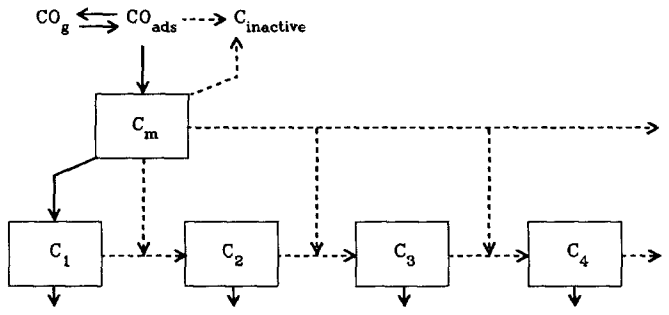

FIG. 1. Isotopic tracing of surface carbon through the CO hydrogenation reaction network. Trajectories traced and exits monitored (solid lines) vs those not observed (dashed lines).

mode of poisoning affecting the amount of hydrogen chemisorbed (*11*).

2.2. *CO Hydrogenation Reaction Analysis*

After *in-situ* H_2 reduction at 400°C, steady-state CO hydrogenation reaction over the catalysts in the series was studied in a quartz, tubular fixed-bed microreactor (3 mm ID) differentially operated at 215°C and ca. 120 kPa using a flow of H_2/CO = 30/10 ml/min. The space velocity through the porous catalyst bed was maintained at about 80 s^{-1}. For further purification, hydrogen (UHP grade, Linde) was passed through a molecular sieve; carbon monoxide gas containing a 5.15% trace of argon (CP grade, Air Products) was passed through an activated charcoal trap to remove potentially formed carbonyls.

The reactor effluent was analyzed for C_1–C_6 hydrocarbon products by gas chromatographic (GC) analysis (Varian, model 3700) using a Porapak Q column and flame ionization detection. Only linear and small amounts of branched alkanes and alkenes were detected. Carbon dioxide was not formed above detectibility limits at the prevailing reaction conditions as determined by GC analysis of the reactor effluent using a Carbosieve II column and a thermal conductivity detector. Methane selectivities (S_{CH4}) are presented on a mass percent basis. Lumped olefin selectivities ($S_{C=}$) are also presented as mass percentages and are based on and normalized with respect to the C_2–C_5 range of hydrocarbon products formed. Hydrocarbon chain-growth probabilities (α_{chain}) were determined from mole-based Schulz–Flory (S–F) plots using a linear regression over carbon numbers three to six. Since the chain-growth probabilities did not vary systematically over time, the reported initial α_{chain}'s are the average value for the first 4 h of reaction. It is noted that for catalysts with high K^+ doping levels there was considerable experimental error in the product analysis due to the low CO conversions obtained over these catalysts. However, in order to be able to fairly compare isotopic transient results, the amount

TABLE 1

Characteristics of K^+-Doped 3 wt% Ru/SiO_2 Catalysts

Catalyst	K/Ru (atomic)	K^+_{added} (μmol/g)	H_{irrev}[b] (μmol/g)	Ru_S[c] (μmol/g)	θ_K[d]
K00	0.00	0.0	110	110	0.0
K01	0.01	3.0	112	112	0.03
K05	0.05	14.8	98	98	0.13
sK10	0.10	29.7	76	76	0.28
K20	0.20	59.4	49	49	0.55

[a] Duplicated from Ref. (*11*).
[b] From static hydrogen chemisorption at room temperature.
[c] Based on an assumption of $H_{irrev}/Ru_S = 1$.
[d] Fraction of Ru surface atoms blocked by K^+ species, assuming all K^+_{added} resides on Ru surface, where one K^+ species blocks one Ru atom. This number is identical to the loss of hydrogen chemisorption ability (*11*).

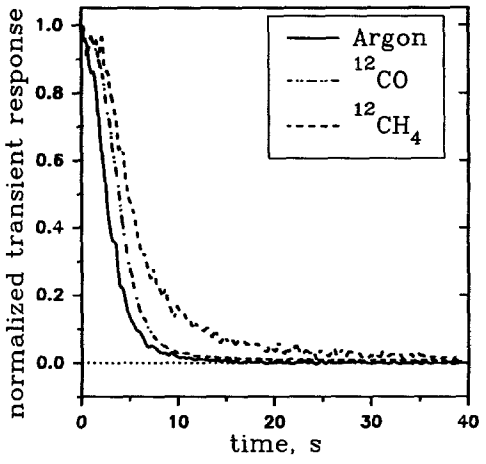

FIG. 2. Typical set of isotopic transients for methane formation during steady-state CO hydrogenation over unpromoted 3 wt% Ru/M5–SiO_2 at standard reaction conditions.

of catalyst in the reactor was kept constant at 60 mg.

In the steady-state isotopic transient kinetic analysis (SSITKA) of methane formation during CO hydrogenation, ^{13}CO (99% enrichment, Isotec) was used without further purification. While the reaction was maintained at steady-state, the decay or development of isotopically marked species was monitored mass-spectrometrically (Extrel, model 275) after abruptly switching between equal flows of labeled-carbon CO in the feed stream without perturbing the reactor pressure. A typical normalized set of isotopic transients is displayed in Fig. 2. Concerning the transients results reported below, it should be noted that for CO the standard deviations of τ and (consequently) N are relatively large because the difference between τ^*_{CO} and τ^*_{Ar} (* indicates the observed decay time, not corrected for gas-phase hold up) tends to be rather small for the transients obtained.

The steady-state isotopic transient technique developed in large part by Happel (*15*) and Biloen (*16*) allows the monitoring of important kinetic parameters under steady-state reaction conditions. For methane formation, the steady-state rate can be written as

$$R_{SS} = N/\tau, \qquad (1)$$

where N is the surface-intermediates abundance and τ is the average surface residence time of these reaction intermediates. Unlike conventional steady-state methods, SSITKA is able to deconvolute the reaction rate into contributions due to the coverage in reaction intermediates vs contributions due to the reactivity of these species. This ability is very powerful since it permits one to address the nature of groups of reaction sites. For conventional nonsteady-state transient techniques which attempt a similar decoupling of the reaction rate, the analysis is complicated by the pressure shock that transpires, which results in a disturbance of the population of surface reaction intermediates during the nonsteady-state transient. For SSITKA, the average intrinsic rate, $\bar{k}$, corresponds inversely to the residence time of the surface reaction intermediates (i.e., $\bar{k} = 1/\tau$) which can be determined from steady-state isotopic transients such as those in Fig. 2. This simplicity cannot be claimed by isotopic pulse methods (*17, 18*).

SSITKA ordinarily does not distinguish between different possible forms of active carbon intermediates since, in fact, it is generally assumed that reaction takes place over a kinetically uniform catalyst surface. However, SSITKA can and has been extended for pseudo-first-order surface reactions to allow the assessment of surfaces that may not be kinetically uniform (*19–21*). To ascertain the effect that potassium may have on different types of surface carbon an extension of SSITKA (the T–F method) described elsewhere (*21*) was used for the nonparametric determination of reactivity distribution functions $f(k)$ from steady-state isotopic transients using a constrained standard Tikhonov regularization of the following Fredholm equation of the first kind,

$$R(t) = N \int_0^\infty k e^{-kt} f(k) dk, \qquad (2)$$

where $R(t)$ is the gas phase-corrected steady-state isotopic transient of methane. The T–F method uses a variant on the approach suggested by Butler *et al.* (*22*) to determine the optimal amount of smoothing needed for the integral inversion.

To determine the effects of catalyst deactivation with time-on-stream (*TOS*), the data-acquisition schedule during CO hydrogenation reaction was as follows. Initial GC product analysis was done after 20 min of reaction since at that time the reaction rates appeared stable, except for the relatively slow catalyst deactivation due to the formation of inactive carbon. Subsequent product analyses could be done at about 40-min intervals and were performed periodically during the catalyst's time-on-stream. In addition, at 20 min on stream the first set of methane transients were measured by continuous mass analysis of the reactor effluent after changing reactants from ^{12}CO to ^{13}CO for a period of 4 min during steady-state reaction. Later sets of such isotopic transients were typically measured at around 80 min, 4 h, 24 h, 48 h, and 72 h on stream.

3. RESULTS

3.1. Initial Reaction

3.1.1. Overall hydrocarbon synthesis. Sequentially added K^+ had a considerable effect on the Ru catalysts' conversion rate of CO (Table 2). There were sharp decreases in both the overall CO conversion rate ($-R_{CO}$) and CO turnover frequency (TOF_{CO}) at low K^+ levels, but at higher doping levels further effects of the promoter on these parameters became less pronounced. Figure 3 shows how CO conversion activity declined as the fraction of surface-exposed Ru($1-\theta_K$) decreased upon addition of K^+. As can be seen in Table 2, the effect of K^+ on S_{CH4} does not appear to have been significant. Likewise, Fig. 4 shows that the initial chain-growth probabilities did not change significantly upon K^+ promotion. Table 2 indicates that the modifier had a significant effect on the lumped C_2–C_5 olefin selectivity ($S_{C=}$), and that S_{CH4} was perhaps more sensitive to higher loadings of K^+.

SSITKA results show that at the prevailing reaction conditions K^+ apparently did not influence τ_{CO} and N_{CO} (Table 2) within experimental error. This CO adsorbed on the catalyst but desorbed without reacting to form CH_4. It should be noted that, within experimental error, N_{CO}'s for the catalysts in the series were similar to or exceeded Ru_S of the unpromoted catalyst (Table 1). We also note that, for the surface residence time and abundance of reversibly adsorbed CO (τ_{CO} and N_{CO}, respectively), averages over time are reported in Table 2 since these parameters did not vary systematically with time.

3.1.2. Methane formation. K^+ addition resulted in sharp decreases in methane production rates (Table 3). Again the promotion effect became progressively smaller with increased doping levels. Figure 5 shows the extent to which the methane activity was decreased due to the addition of the modifier whether expressed as R_{CH4}, TOF_{CH4}, or k_{CH4}. The figure illustrates that as one can get more site specific about the methane-formation activity, the influence of K^+ on the activity seems to be less, which indicates that the promoter must also have been affecting the abundance of reaction intermediates, as is the case and as shown in Table 3. Table 3 indicates that, if it is assumed that the CH_X coverage of surface Ru is one-to-one, then the methane-destined surface intermediates would correspond to an overlayer covering 9% of the Ru surface atoms for the K^+-free catalyst, with this overlayer coverage decreasing to 2% of the substrate metal surface for the catalyst with the highest K^+ doping level.

The nonparametric T–F estimates of the reactivity distributions are shown in Fig. 6 and were extracted from isotopic transients measured after 20 min at standard reaction conditions. To facilitate their comparison, each distribution has been rescaled to reflect that the total steady-state number of methane-destined surface carbon atoms was

TABLE 2

Initial[a] Overall CO Hydrogenation Reaction Characteristics

Catalyst	Conv. (%CO)	$-R_{CO}$ (μmol/g s)	TOF_{CO}[b] (10^{-3} s^{-1})	S_{CH4} (wt%)	$S_{C=}$ (wt%)	τ_{CO}[c,d] (s)	N_{CO}[c,e] (μmol/g)
K00	4.1	5.1	46	49	30	1.1	140
K01	2.7	3.4	30	53	30	0.8	100
K05	0.65	0.81	8	58	60	1.4	170
sK10	0.36	0.32	4	48	80	1.3	160
K20	0.15	0.18	4	39	70	0.9	110

[a] Values after 20 min of reaction.
[b] $TOF_{CO} \equiv -R_{CO}/H_{irrev}$.
[c] Average over time; values did not vary systematically over time.
[d] Standard deviation is 0.3 s.
[e] Standard deviation is 40 μmol/g.

N_{CH4}. The relative smoothness of the T–F estimates is a direct consequence of the Tikhonov regularization approach, and any random experimental error in the measurement of the isotopic transients would be primarily reflected as uncertainty about peak locations of the true reactivity functions. For the transformed isotopic transients, such uncertainty is expected to be modest since the noise in the transient measurements is estimated to have been small (between 2 and 6%). For the transient of the K20 catalyst, the level of noise relative to the low methane-formation activity was too great to allow a reliable estimate of the reactivity spectrum using the T–F method.

Figure 6 shows that on this series of Ru/SiO_2 catalysts the formation of methane during steady-state CO hydrogenation was regulated by two reaction trajectories for methane-destined carbidic carbon. The highly reactive pool is assigned $C_{1\alpha}$ and the less reactive one $C_{1\beta}$. These methane-destined carbon pools are only a part of the larger C_α and C_β pools (*19, 23*) which yield both methane and higher hydrocarbons (C_{2+}). As can be seen in Fig. 6, small amounts of alkali seem to have primarily affected the $C_{1\alpha}$ pool, but higher levels of sequentially added potassium affected both

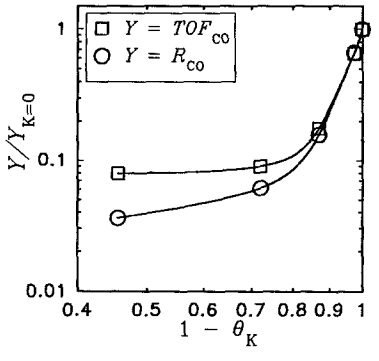

FIG. 3. Potassium-induced changes in CO conversion activity vs exposed surface ruthenium ($1-\theta_K$).

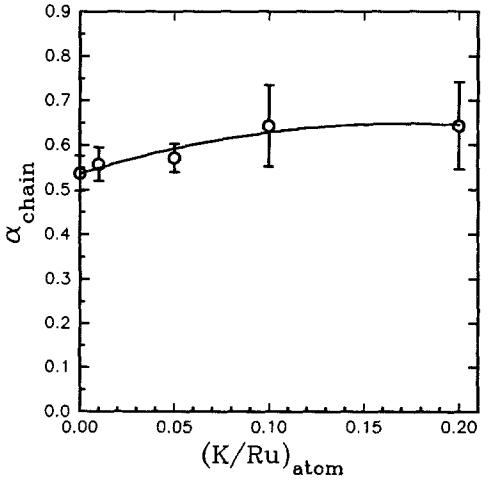

FIG. 4. Potassium-induced shifts in the hydrocarbon chain-growth probability.

TABLE 3

Initial[a] Methane Formation Characteristics

Catalyst	R_{CH4} (μmol/g s)	TOF_{CH4}[b] (10^{-3} s^{-1})	τ_{CH4}[c,d] (s)	$\bar{k}_{CH4}$[c] (s^{-1})	N_{CH4} (μmol/g)	θ_{CH4}[e]
K00	2.51	23	4.2	0.24	9.4	0.086
K01	1.80	16	4.0	0.25	7.4	0.065
K05	0.47	4.8	6.9	0.14	3.3	0.029
sK10	0.15	2.0	14	0.07	2.1	0.020
K20	0.07	1.4	34	0.03	2.4	0.022

[a] Value after 20 min of reaction.
[b] Based on static chemisorption of irreversible hydrogen.
[c] Average over time; values did not vary systematically with time. Equal to $1/\tau_{CH4}$.
[d] Standard deviation is 0.5 s.
[e] Fraction of Ru surface atoms covered by CH_x. Normalization with respect to Ru_S of K^+-free catalyst (K00) and based on the assumption that $CH_x/Ru_S = 1$.

pools considerably. In addition, there was a considerable decrease in the reactivity of $C_{1\alpha}$ although in relative terms it was similar to the decrease seen for $C_{1\beta}$. Table 4 shows that K^+ decreased the methane-destined $C_{1\alpha}$ population to a slightly greater extent than that of $C_{1\beta}$.

It is also possible to assess the contribution of the active carbon pools to the overall methane formation rate. If $f(k)$ corresponds to the steady-state fraction of active CH_4 intermediates on the catalyst surface which each have reactivity k, then $kf(k)$ corresponds to the extent at which this group of carbon atoms reacts to contribute to overall methane production. Table 5 shows the extent to which the contribution of the active surface carbon pools to the formation of methane was affected by added K^+. For the K^+-free catalyst, $C_{1\beta}$ corresponded to 40% of the steady-state abundance in the methane-destined portion of the carbidic adlayer, but it contributed to only 5% of the observed methane formation rate. Addition of K^+ to the catalyst led to increases in the relative contribution (x') of $C_{1\beta}$ to the decreasing rate

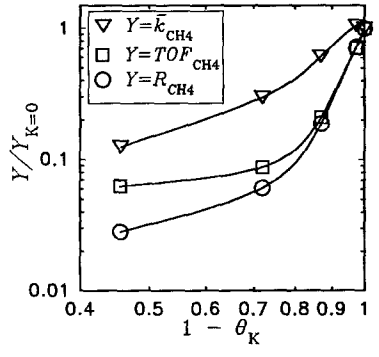

FIG. 5. Potassium-induced changes in methane-formation activity vs surface-exposed ruthenium.

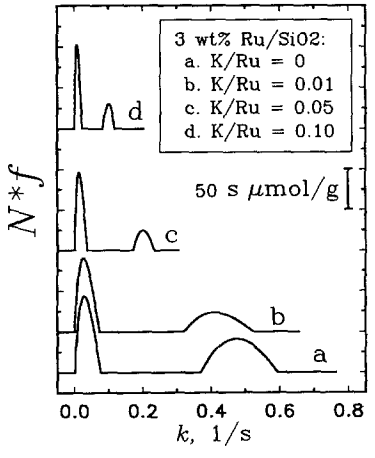

FIG. 6. K^+-induced shifts in the reactivity spectrum for active carbon on Ru/SiO_2. $Nf(k)$ represents the absolute density of CH_4-destined C of reactivity k.

TABLE 4

Initial Sizes of Methane-Destined Active Carbon Pools and Their Average Reactivities

Catalyst	$\bar{k}_{C1\beta}$ (s^{-1})	$N_{C1\beta}$ (μmol/g)	$\bar{k}_{C1\alpha}$ (s^{-1})	$N_{C1\alpha}$ (μmol/g)	$\bar{k}_{C1\alpha}/\bar{k}_{C1\beta}$
K00	0.035	4.1	0.48	5.3	14
K01	0.033	4.3	0.42	3.1	13
K05	0.017	2.3	0.20	0.99	12
sK10	0.010	1.4	0.10	0.66	10

of methane formation due to the relatively greater suppression of both the surface concentration and reactivity of $C_{1\alpha}$.

3.2. Catalyst Deactivation

Figure 7 shows that for all the catalysts in the series the CO conversion rate decreased with time-on-stream, with the most pronounced deactivation occurring over the first 24 h. It appears that upon promotion with K^+, catalyst deactivation by inactive carbon was similar based on a comparison of the relative CO conversion rates, although in absolute terms it was much less.

Figure 8 shows that for the catalyst series, olefin selectivities varied only slightly with time-on-stream (*TOS*). In addition, deactivation of these catalysts had no significant effect on α_{chain} which appeared invariant with *TOS*, but there were minimal increases in S_{CH4} with *TOS*. However, with time, the rates of methane formation of the catalysts in the series (Fig. 9) were affected similarly as the CO conversion rates (Fig. 7).

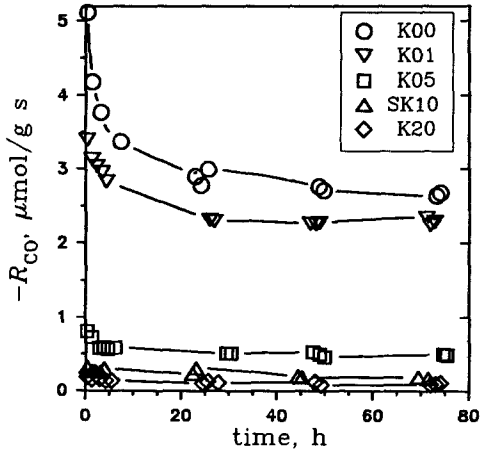

FIG. 7. Time-on-stream CO conversion rates.

As noted in Table 3, SSITKA indicates that for the catalysts in the series $\bar{k}_{CH4}$ remained constant with *TOS* so that, at least for methane formation, the loss in activity can be wholly attributed to a steady loss in the number of active, carbon-containing surface intermediates (see Fig. 10). It is noted that an approach based on the traditionally used *TOF* would have incorrectly attributed the CH_4 rate decline upon carbon deactivation to a decrease in site activity.

4. DISCUSSION

4.1. Potassium Promotion of Initial Synthesis

Alkali-induced effects on CO hydrogenation, regardless of how they may actually come about, have been reported often (*1*, *24–30*) and were also observed in this study

TABLE 5

Initial Relative Contributions of Methane-Destined Active Carbon Pools to the Reaction (x')

Catalyst	$x'_{C1\beta}$	$x'_{C1\alpha}$
K00	0.05	0.95
K01	0.10	0.90
K05	0.16	0.84
sK10	0.18	0.82

Note. $x' = kf(k)$.

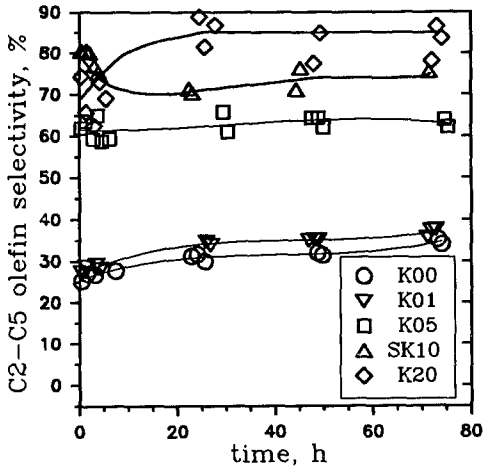

FIG. 8. Time-on-stream olefin selectivities.

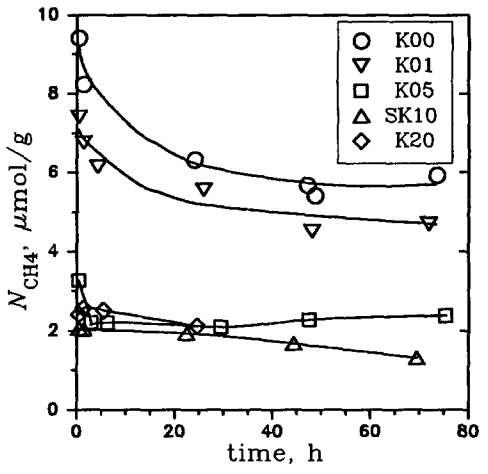

FIG. 10. Time-on-stream methane precursor abundances.

(Table 2). The SSITKA results reported in Table 3 confirm that the alkali indeed works to decrease the average reactivity of at least the surface carbon that reacted to form methane. At the same time SSITKA also shows an alkali-induced decrease in the steady-state amount of this surface carbon (Table 3), but at this point it is not altogether clear how such a decrease may have come about. In the context of the electrostatic approach mentioned in the introduction, one may suggest that even though surface carbon is more readily formed due to increased CO dissociation, it becomes more difficult to hydrogenate this more tightly bound carbon. Thus, the surface may be more covered by inactive carbon which would not be detected by SSITKA.

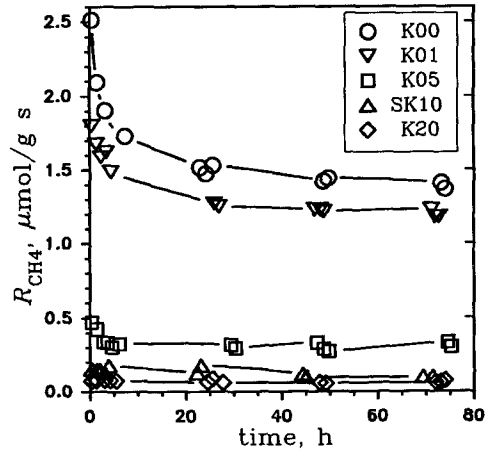

FIG. 9. Time-on-stream rate of methane formation.

The alkali-promotion mechanism mentioned earlier above may not be complete since for a long time it has been known that the carbidic layer most likely consists of several kinds of surface carbon which have different reactivities (*31*). In fact, the reactivity spectra in Fig. 6 suggest that incorporation of surface carbon into methane occurs via two separate main pathways distinguished by different carbon intermediates or different site–carbon interactions. Since it can be extremely difficult to identify different forms of carbon (*8*), especially during reaction conditions, we will first attempt to make inferences about the effect of K^+ on these pools based solely on the kinetic information available from the experiments and broadly accepted views of how alkali species influence metal surfaces and coadsorbates. Subsequently, the possible nature of the two surface carbon pools will be addressed in light of our findings.

4.1.1. Modification of carbon pathways. On Ru, the dissociation of CO is fast compared to the hydrogenation of surface carbon (*32, 33*). Thus, even though K^+ enhances the rate of CO dissociation, this

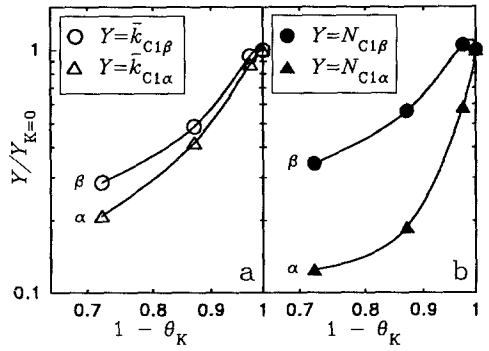

FIG. 11. Extent of alkali-induced variation in the reactivity (a) and abundance (b) of active surface carbon pools vs surface-exposed ruthenium.

dissociation process is probably less important in the consideration of the K^+ modification of the reaction. Instead, it is kinetically more important to focus on possible K^+ modification of other processes such as the hydrogenation, chain growth, and deactivation of surface carbon.

As indicated by Fig. 6, the two observed trajectories for the hydrogenation of surface carbon to methane *shifted gradually* to lower reactivities with increasing levels of K^+. This signifies that promotion did not alter the reaction mechanisms involved. If alternative paths were possible upon promotion, one would expect additional peaks to appear in the reactivity spectrum while the original ones were attenuated. This was not the case. Thus, it appears that the two methane-destined trajectories of surface carbon were only modified by having their rates decreased.

It may not be entirely appropriate to explain the site requirements of the two carbon pools as they are hydrogenated based on the results shown in Fig. 11. This is especially so since in order to account for the influence of K^+ on the size of the $C_{1\alpha}$ and $C_{1\beta}$ pools one has to consider several issues simultaneously, including: (i) the geometric site blocking effect of the modifier, (ii) possible K^+-induced self-poisoning by unreactive carbon C_γ, (iii) possible reaction ensemble effects, and (iv) the surface mobility of reaction intermediates. This is why Biloen *et al.* (*34*) pointed out the distinction that should be maintained between SSITKA-derived information on reaction intermediates and inferences made about reaction sites that these intermediates may be associated with. Thus, addressing the underlying reaction sites requires more information or additional assumptions.

In order to address the modification of reaction sites, it is often tacitly assumed that one surface intermediate species occupies one active metal atom and is laterally constrained; i.e., a single-atom reaction ensemble approach is used. In certain situations it is possible to use a statistical approach (*35*) to estimate the required reaction ensemble size from poisoning experiments if it can be assumed that the catalyzing surface is kinetically uniform and the poison brings about only site blocking. However, it is evident that assuming uniform surface kinetics or inert poisoning would be inappropriate in the case of methane formation during K^+-promoted CO hydrogenation since the alkali dopant modifies the reactivity of the carbon pools (Fig. 11a) and it cannot be considered to be an inert poison. Therefore, it is not possible to determine site requirements from Fig. 11b since K^+ affected the N_{C1}'s *both* by simple site blocking and by decreasing the intrinsic hydrogenation rate of surface carbon.

Based on spectroscopic and MO studies available to date (*8, 31, 32, 36–43*), we are not able at this point to identify with confidence the nature of the surface carbon involved in the two main reaction pathways suggested by the reactivity spectra. In their SSITKA study of methanation on Ni, Soong *et al.* (*23*) also predicted two main pathways for the incorporation of surface carbon into methane but they did not attempt to identify the nature of these reaction trajectories. The SSITKA-derived reactivity distributions for Ru- and Ni-catalyzed methane formation in a study by de Pontes *et al.* (19) also suggested two main reaction pathways for surface carbon. It is tempting to follow the ex-

ample of de Pontes *et al.* (*19*) and assign the high-reactivity surface carbon pool to carbidic carbon and the low-reactivity one to short alkyls found in NMR studies by Winslow and Bell (*32, 33*). In these latter studies (*32, 33*) two species were identified during CO hydrogenation and the results indicate carbidic carbon to be more reactive than short alkyls upon TPSR with hydrogen. However, in our case such an assignment may be considered arduous in light of the following concerns.

Firstly, the NMR results (*32*) show that some adsorbed alkyls regress to carbidic carbon atoms only after the reaction is interrupted by flushing the reactor with an inert gas. These results do not indicate that during CO hydrogenation the short alkyls undergo hydrogenolysis to form methane. In fact, it is likely that during CO hydrogenation, adsorbed alkyls react to form alkanes or alkenes since hydrogenolysis is prohibited due to acute CO poisoning of the latter pathway (*10*). Thus, even though it has been shown that some C_1 fragments of ethene can be incorporated into propene when considerable concentrations of ethene are co-fed during syngas conversion (*44*), adsorbed alkyls should probably not be viewed as a potential carbon reservoir for the more reactive carbidic surface carbon pool leading to methane during CO hydrogenation.

Secondly, if one considers that the fraction $C_{1\beta}$ in the reactivity spectrum are adsorbed methyls, there would be a conflict with the fact the $C_{1\alpha}$ pool is more reactive than the $C_{1\beta}$ one. That is, there seems to be no apparent reason why CH_3 would be hydrogenated more slowly than multiply-bound surface carbide since the carbon in the latter species would have to pass through a CH_3 state in order to form methane. In light of these concerns, it is not easy to accept that $C_{1\alpha}$ and $C_{1\beta}$ signify carbon intermediates leading to methane which are carbidic carbon and short alkyls, respectively.

An alternative assignment of the carbon pools, based on predictions from MO theory (*39–41*) is also arduous. This approach would specify that carbidic carbon is hydrogenated to form methane by both a surface carbide route

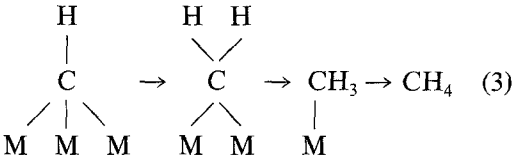

(3)

and a terminal-carbene one

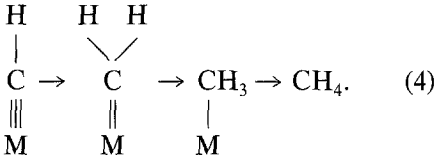

(4)

Using this approach, reaction via the carbide route is considered to be slower than by the carbene one because surface carbides are predicted to be more stable as indicated by their typically lower total energies (*39–41, 45, 46*). It should be noted that there is spectroscopic evidence which indicates the existence of surface carbides (*47, 48*). However, it remains a question whether or not terminal carbenes would be stable enough to exist as rate-determining surface intermediates at typical CO hydrogenation reaction conditions.

Furthermore, using the carbide/carbene path assignment, one would expect that surface carbides would suffer more from the alkali's action since, as suggested by the electrostatic approach, they may be influenced by K^+ adspecies through more than one metal atom. Thus, while the carbide/carbene assignment would be compatible with the observed decreases in $\bar{k}_{C1\alpha}$ and $\bar{k}_{C1\beta}$ upon promotion, it is not able to account for the concurrent decrease in the $\bar{k}_{C1\alpha}/\bar{k}_{C1\beta}$ ratio (Table 4). Of course, as discussed earlier, it is likely that it is inherently more difficult to further stabilize the relatively more stable rate-controlling intermediate species of the less reactive $C_{1\beta}$ pool. Even so, in light of the uncertainty about so many critical points, the surface carbide/carbene assignment remains unsatisfactory.

Thus, the SSITKA results are not able to shed more light on the chemical nature of the surface intermediates, other than to delineate their kinetic differences.

4.2. *Catalyst Deactivation by Carbon*

For all the catalysts in the series, the reaction results suggest that even though overall catalyst activity decreases with *TOS*, catalyst deactivation did not seriously affect the product distribution at the prevailing reaction conditions. It is noted that since no CO_2 was detected in the reactor effluent, carbon deposition via the Boudouard reaction is not a concern. There were, with time, some slight improvements in the olefin selectivity (Fig. 8) which would indicate a decrease in the hydrogenation rate upon deactivation. On the other hand, with time there were slight increases in S_{CH4} (Table 2). However, other critical selectivity parameters such as α_{chain} and $\bar{k}_{Ch4}$ did not change significantly during 3 days on stream. This offers the possibility that the observed, slight changes in $S_{C=}$ and S_{CH4} may be trivial and that under the prevailing reaction conditions the product distribution did not change significantly despite the deactivation. It has been reported often that with *TOS* the product distribution changes to reflect a decrease in the hydrogenation rate (*49*). However, it has also been observed that under certain conditions the product distribution is not affected by deactivation, especially if the synthesis gas is not hydrogen deficient (*49, 50*), as was the case here with $H_2/CO = 3$.

From the results it is not entirely clear how during catalyst deactivation transformation of active carbon into unreactive C_γ may have taken place. Since at the prevailing reaction conditions $\bar{k}_{CH4}$ remained constant with TOS for the catalysts in the series, deactivation does not appear to have affected the intrinsic hydrogenation rate of the methane-destined carbidic intermediates. This suggests that catalyst deactivation was entirely due to site blockage by unreactive C_γ, with the hydrogenation of active carbon intermediates on the unblocked sites continuing unperturbed. Note that the relatively time-invariant product distribution also supports the last suggestion.

Since C_γ does not appear to have altered the intrinsic hydrogenation/removal rate of active carbon intermediates, the fact that for the catalysts in the series N_{CH4} declined to a steady-state value (Fig. 10) signifies that there must have been a decline in the overall formation/deposition rate of active carbon. It is unlikely that the intrinsic rate of formation of nascent carbon would be significantly affected by neighboring C_γ. The observed decreases in N_{CH4} with time (Fig. 10) therefore imply that the intrinsic deposition rate of nascent carbon may not be the same on all metal sites. There are indications that on single crystals of Ru, CO dissociation occurs preferentially on stepped surfaces, and that the resulting C–M bonding of surface carbon is stronger near the steps (*51, 52*). It therefore seems likely that on such sites of stronger C–M bonding, which also have a higher intrinsic rate of carbon formation before being poisoned, C_γ is apt to form more readily. Once these sites which form carbon too fast have been self-poisoned by C_γ, a steady state is eventually reached in the abundance of active carbon intermediates on the remaining sites as indicated in Fig. 10. Thus, for the remaining active carbon intermediates a kinetic equilibrium would be reached in which the intrinsic rates of formation/deposition and hydrogenation/removal are equal, with the latter rate controlling the kinetics. Such a kinetic equilibrium may possibly explain a Fischer–Tropsch study of Ru which showed that after a short induction period there was no catalyst deactivation, as indicated by stable hydrocarbon production rates over a period of six months (*53*).

The specific influence that K^+ may have had on catalyst deactivation is not entirely clear from our results. The decrease in $\bar{k}_{CH4}$ upon promotion may indicate that K^+ increased the C–M bond strength of the surface so that there was initially less reactive carbidic carbon available for hydrogenation

upon promotion. As indicated by Fig. 10, at initial reaction fewer reaction sites/intermediates remained active (at somewhat lower reactivity) upon promotion. It is possible that most of those sites which tended to deactivate were already lost initially due to the excessive C–M bonding induced by K^+. This would mean that upon promotion the C_γ adlayer may have been larger at "initial" reaction conditions as defined here (20 min on stream). It is clear that such an interpretation would not require any additional functions for K^+ beyond those that were observed at initial reaction.

5. CONCLUSIONS

Potassium-promoted, Ru-catalyzed CO hydrogenation and its deactivation by carbon were studied using conventional steady-state reaction analysis augmented by SSITKA of methane-destined surface carbon. The steady-state product analysis showed that upon K^+ promotion there was a general increase in the hydrocarbon chain-growth probability and the olefin selectivity. Such results are typical of what others have observed before (*26, 27*).

SSITKA indicates that during CO hydrogenation the incorporation of carbidic carbon into methane was regulated by two surface trajectories: a high-reactivity path ($C_{1\alpha}$) and a low-reactivity one ($C_{1\beta}$). Upon alkali promotion both the $C_{1\alpha}$ and $C_{1\beta}$ pools were held up longer on their respective trajectories while their steady state abundances also decreased. Both in terms of its reactivity and abundance, the $C_{1\alpha}$ pool was affected to a slightly greater extent than the less reactive $C_{1\beta}$ one. The results are consistent with the view that on dispersed Ru catalysts, alkali modifiers increase metal–carbon bonding which leads to a reduction in the hydrogenation rate of surface carbon intermediates.

Product analysis indicates that at prevailing reaction conditions on a *relative* basis K^+ did not appear to have stabilized catalyst activity with time-on-stream; however, on an absolute basis, there were differences. For all the catalysts in the series, the overall product distribution did not vary significantly with *TOS*, and SSITKA revealed that, for these sequentially doped, K^+-promoted Ru/SiO_2 catalysts, the average *intrinsic* turnover frequency of the sites producing methane ($\bar{k}_{CH4}$) did not vary with time-on-stream. This suggests that unreactive carbon did not bring about site modification; rather, it only resulted in simple site blocking.

ACKNOWLEDGMENTS

The work presented here had the financial support of the National Science Foundation (Grant CBT-8715541). One of us (T.E.H.) also thanks the Texaco Foundation for one of its graduate fellowships.

REFERENCES

1. Anderson, R. B., *Catalysis* **4,** 29 (1956).
2. Dry, M. E., Shingles, T., Boshoff, L. J., and Oosthuizen, G. J., *J. Catal.* **15,** 190 (1969).
3. Dry, M. E., Shingles, T., and Boshoff, L. J., *J. Catal.* **25,** 99 (1972).
4. Biloen, P., private communication, 1986.
5. Bonzel, H. P., *Surf. Sci. Rep.* **8,** 43 (1987).
6. Nørskov, J. K., Holloway, S., and Lang, N. D., *Surf. Sci.* **137,** 65 (1984).
7. Uram, K. J., Ng. L., and Yates, J. T., Jr., *Surf. Sci.* **177,** 253 (1986).
8. Joyner, R. W., *Vacuum* **38,** 309 (1988).
9. Wang, J., M.S. Thesis, University of Pittsburgh, Pittsburgh, PA, 1990.
10. Storch, H. H., Columbic, N., and Anderson, R. A., "The Fischer–Tropsch and Related Synthesis." Wiley, New York, 1951.
11. Hoost, T. E., and Goodwin, J. G., Jr., *J. Catal.* **130,** 283 (1991).
12. Angevaare, P. A. J. M., Hendrickx, H. A. C. M., and Ponec, V., *J. Catal.* **110,** 11 (1988).
13. Angevaare, P. A. J. M., Hendrickx, H. A. C. M., and Ponec, V., *J. Catal.* **110,** 18 (1988).
14. Iyagba, E. T., Hoost, T. E., Nwalor, J. U., and Goodwin, J. G., Jr., *J. Catal.* **123,** 1 (1990).
15. Happel, J., *Chem. Eng. Sci.* **33,** 1567 (1978).
16. Biloen, P., *J. Mol. Catal.* **21,** 17 (1983).
17. Biloen, P., and Sachtler, W. H. M., *Adv. Catal.* **30,** 165 (1981).
18. Cant, N. W., and Bell, A. T., *J. Catal.* **73,** 257 (1982).
19. de Pontes, M., Yokomizo, G. H., and Bell, A. T., *J. Catal.* **104,** 147 (1987).
20. Nwalor, J. U., Ph.D. Dissertation, University of Pittsburgh, Pittsburgh, PA, 1988.
21. Hoost, T. E., and Goodwin, J. G., Jr., *J. Catal.* **134,** 678 (1992).

22. Butler, J. P., Reeds, J. A., and Dawson, S. V., *SIAM J. Numer. Anal.* **18,** 381 (1981).
23. Soong, Y., Krishna, K., and Biloen, P., *J. Catal.* **97,** 330 (1986).
24. Huang, C. P., and Richardson, R. J., *J. Catal.* **51,** 1 (1978).
25. McVicker, G. B., and Vannice, M. A., *J. Catal.* **63,** 25 (1980).
26. Gonzalez, R. D., and Miura, H., *J. Catal.* **77,** 338 (1982).
27. McClory, M. M., and Gonzalez, R. D., *J. Catal.* **89,** 392 (1984).
28. Chai, G.-Y., and Falconer, J. L., *J. Catal.* **93,** 152 (1985).
29. Blackmond, D. G., Williams, J. A., Kesraoui, S., and Blazewick, D. S., *J. Catal.* **101,** 496 (1986).
30. Rieck, J. S., and Bell, A. T., *J. Catal.* **100,** 305 (1986).
31. McCarty, J. G., and Wise, H., *J. Catal.* **57,** 406 (1979).
32. Winslow, P., and Bell, A. T., *J. Catal.* **86,** 158 (1984).
33. Winslow, P., and Bell, A. T., *J. Catal.* **94,** 385 (1985).
34. Biloen, P., Helle, J. N., van den Berg, F. G. A., and Sachtler, W. M. H., *J. Catal.* **81,** 450 (1983).
35. Martin, G. A., *Catal. Rev.-Sci. Eng.* **30,** 519 (1988).
36. Dost, A. A., Dhanak, V. R., and Bassett, D. W., *Vacuum* **33,** 687 (1983).
37. Dost, A. A., Dhanak, V. R., and Buckingham, S., *J. Catal.* **89,** 159 (1984).
38. Yokomizo, G. H., and Bell, A. T., *J. Catal.* **119,** 467 (1989).
39. Minot, C., van Hove, M. A., and Somorjai, G. A., *Surf. Sci.* **127,** 441 (1982).
40. Zheng, C., Apeloig, Y., and Hoffmann, R., *J. Am. Chem. Soc.* **110,** 749 (1988).
41. de Koster, A., and van Santen, R. A., *J. Catal.* **127,** 141 (1991).
42. Gavin, R. M., Jr., Reutt, J., and Muetterties, E. L., *Proc. Natl. Acad. Sci. U.S.A.* **78,** 3981 (1981).
43. Schüle, J., Siegbahn, P., Wahlgren, U., *J. Chem. Phys.* **89,** 6982 (1988).
44. Percy, L. T., and Walter, R. I., *J. Catal.* **121,** 228 (1990).
45. Muetterties, E. L., *J. Organomet. Chem.* **200,** 177 (1980).
46. Fox, D. J., and Schaeffer, H. F., III, *J. Chem. Phys.* **28,** 328 (1983).
47. McBreen, P. H., Erley, W., and Ibach, H., *Surf. Sci.* **148,** 292 (1984).
48. Duncan, T. M., Winslow, P., and Bell, A. T., *J. Catal.* **93,** 1 (1985).
49. Ponec, V., *Coal Sci.* **3,** 1 (1984).
50. Agrawal, P. K., Katzer, J. R., and Manogue, W. H., *J. Catal.* **69,** 321 (1981).
51. Shincho, E., Egawa, C., Naito, S., and Tamaru, K., *Surf. Sci.* **149,** 1 (1985).
52. Shincho, E., Egawa, C., Naito, S., and Tamaru, K., *Surf. Sci.* **155,** 153 (1985).
53. Pichler, H., *Adv. Catal.* **4,** 271 (1952).